Microstructure and Property of Sintered Fe-2Cu-0.8C-0.6Mo-2W Materials Prepared From Prediffused Powders

Wenchao Chen[1,2], Jinghui Wang[1,2], Pengqi Chen[1,2] and Jigui Cheng[1,2]*

[1]School of Materials Science and Engineering, Hefei University of Technology, Hefei, China, [2]Research Centre for Powder Metallurgy Engineering and Technology of Anhui Province, Hefei, China

Prediffused Fe-W powder with 2 wt% of tungsten was prepared by heating Fe-W powder mixes at 800°C for 45 min in H_2 atmosphere. Two kinds of Fe-2Cu-0.8C-0.6Mo-2W powder mixtures were obtained by mechanically mixing the prediffused Fe-W powders with the other elemental powders. After pressing and sintering, the sintered Fe-2Cu-0.8C-0.6Mo-2W materials were obtained from the two powder mixtures. The effects of the introducing methods of tungsten element and sintering conditions on microstructure, mechanical and wear properties of the sintered samples were investigated. The results show that with the increase of sintering temperature and time, hardness and strength of sintered samples increase. Prediffused treatment of Fe-W powder can improve density of green compacts and sintered samples. When W element introduced in the form of prediffused Fe-W powders, the compacts pressed at 700 MPa have a green density of 7.13 g/cm³, and after sintered at 1,150°C, the density, hardness, tensile strength and radial crushing strength of the sintered samples are 7.16 g/cm³, 95 HRB, 547 and 791 MPa, respectively, which are higher than those of the samples prepared from powder mixtures by mechanically mixing the elemental powders. Furthermore, the prediffused treatment of Fe-W powders can improve the distribution of W element and enhance wear resistance.

Keywords: ferrous powder metallurgy, prediffused Fe-W powders, sintering, microstructure, property

INTRODUCTION

Iron-copper-carbon (Fe-Cu-C) alloy is the most widely used sintered iron-based materials, accounting for more than 50% of in the sintered ferrous powder metallurgy parts (Lee et al., 2012; Annamalai et al., 2013; Azevedo et al., 2018). With the developments of modern industry and manufacturing technology, the performance of sintered ferrous components is more required rigorously. Researchers have found that the performance can be improved by adding alloying elements, such as Mo, Ni, and Cr and so on. These elements not only have the effect of solution strengthening, but can also refine the grain size of pearlite. (Wu et al., 2016; Wang et al., 2019; Zhang et al., 2019). Among these, tungsten as a novel alloying element has an excellent hardening effect, which can be used to enhance the matrix and improve the high temperature strength (Deng et al., 2014; Xuan et al., 2019). The sintered PM materials with W addition show good wear resistance due to the forming of carbides (Silva et al, 2009), and reduce the stress concentration at high temperature

(Meng et al., 2020). However, the particle size of tungsten elemental powders used in PM process is almost smaller than of the raw iron powders, and the density difference between W and Fe is large. During mixing it is easy to agglomerate and segregate, resulting in non-uniformity of element distribution in both powder mixtures and sintered materials (Daumann et al., 2011; Aditya et al., 2015; Oka et al., 2017). Therefore, an investigation toward introducing new methods for alloying powders and the preparation process has significance in promoting application for W-containing ferrous PM materials.

Nowadays, researchers have tried to introduce alloying elements in some other forms to improve the homogeneity and process properties of the powder mixtures (Narasimhan, 2001; Cristofolini et al., 2018). One such approach, known as adding predebuffered powders, is an effective way to realize the improvement of PM industry (Semel, 1990; Xiao et al., 2009; Lee et al., 2012). The main advantages of predebuffered powders compared to mechanically mixing powder mixtures and prealloyed powders are better fluidity and bulk density, uniform alloy elements distribution, and microstructure homogeneity, which can improve performance and consistency of sintered parts (Chawla et al., 2001; Wu et al., 2013; Pope et al., 2019). On the other hand, predebuffered powders usually contain Ni, Mo, and Cu elements, but the preparation of W-containing predebuffered powders and their sintering properties are rarely reported.

In this paper, predebuffered Fe-W powders were prepared by predebuffered treatment, Fe-2Cu-0.8C-0.6Mo-2W powder mixtures were then obtained by mechanically mixing the predebuffered Fe-W powders with the other elemental powders (PD powder mixtures), and for comparison, mechanically-prepared powder mixtures were prepared by mechanically mixing all the elemental powders (EL powder mixtures). The sintered Fe-2Cu-0.8C-0.6Mo-2W materials with different methods of introducing tungsten and sintering processes were prepared subsequently. The microstructure, mechanical and wear properties of sintered samples were systematically tested to investigate the effects of W addition forms on properties of the sintered samples.

EXPERIMENTAL

Sample Preparation
Preparation of the Predebuffered Fe-W Powder
Reduced iron powders (average particle size of 75 μm) and ultrafine tungsten powders were used as raw materials. The tungsten powders have an average particle size of about 0.8 μm and near spherical shape. Tungsten and iron powders were mixed in a double-cone mixer in air for 20 min. The mechanically mixed powders were then heat treated with a pipe furnace at 800°C for 45 min in H_2 atmosphere. After being crushed and screened through a 100 mesh sieve, the predebuffered Fe-W powder were obtained subsequently.

Preparation of the Sintered Fe-2Cu-0.8C-0.6Mo-2W Samples
Reduced iron powders, water atomized copper powders (average particle size of 32 μm), molybdenum powders (average particle

size of 12 μm), flaky graphite powders (average particle size of 28 μm) and tungsten powders were used as raw materials. Two kinds of Fe-2Cu-0.8C-0.6Mo-2W powder mixtures were obtained by mixing the predebuffered Fe-W powder with the other elemental powders, and mixing all the elemental powders, respectively. Zinc stearate powders were added into the powder mixtures with an addition amount of 0.6 wt% as lubricant. After compaction under 500–700 MPa uniaxially, the green compacts were sintered at 1,050–1,200°C for 60–100 min in H_2 atmosphere without pressure.

## Characterization of the Powders and Sintered Samples
The microstructure and tungsten element distribution of powders and sintered samples were carried out by using a scanning electron microscope (SEM) and energy-dispersive spectroscopy (EDS). Density of the green compacts and sintered samples was measured by the Archimedes' method according to ASTM B328-2003 standards. For sintered samples, the tensile strength test was performed by using a universal material testing machine by the dumbbell specimen with a length of 90 mm at a crosshead speed of 0.5 mm/min. The hardness was measured by using the rockwell hardness tester under a load of 100 kg at room temperature. The radial crushing strength was measured by using the pendulum impact testing machine under a load of 401.93 Nm. Wear tests were carried out by an end face wear tester, Cr12 with a hardness of 58–60 HRC was used as a counter-part with oil lubrication, the fixed load was 100 N, the plate rotated was 1 m/s and the test time was 5 min.

RESULTS AND DISCUSSION

Microstructure and Property of the Powders
Figure 1 shows SEM images of the raw iron, tungsten powders, and predebuffered Fe-W powders with EDS result and XRD patterns of predebuffered Fe-W. The predebuffered powders have an average particle size of about 75 μm (**Figures 1C**), which is the same as that of raw iron powder (**Figures 1A**), so the predebuffered treatment process had no effect on the particle size. It also can be seen that small tungsten particles (raw particles as show in **Figures 1B**) attached to the iron particles, which have a homogeneous distribution with less segregation (**Figures 1D**) in the predebuffered powders. As shown in **Figures 1E**, the EDS analysis confirms that the superfine tungsten particles attached to iron particles. **Figures 1F** shows the XRD patterns of the Fe and predebuffered Fe-W powders. The patterns can be indexed for W (JCPDS No. 47-1319, marked by black squares) and Fe (JCPDS No. 50-1275, marked by white squares). Only diffraction peaks (110), (200), (211) of Fe and (110) of W are observed in **Figures 1F**, and the peaks of predebuffered Fe-W powders shifted slightly due to the solid solution of tungsten element. The predebuffusion treatment promotes partial diffusion of tungsten and iron, which can make small particles of tungsten adhere firmly and avoid segregation.

Figure 2 shows green density of Fe-2Cu-0.8C-0.6Mo-2W compacts by pressing different powder mixtures. It shows that
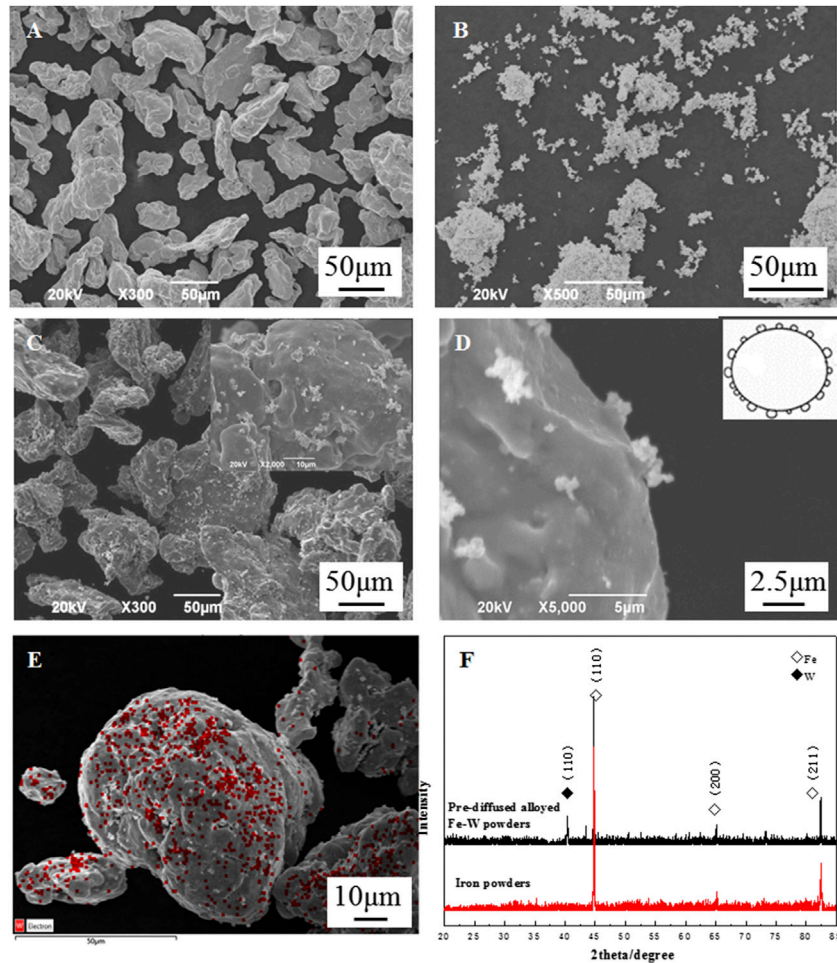
FIGURE 1 | SEM images of iron powders **(A)**, tungsten powders **(B)** and prediffused Fe-W powders **(C, D)**; EDS results **(E)** and XRD patterns **(F)** of prediffused Fe-W powders.

the prediffused treatment influences the compressibility of PD powder mixtures, and a maximum green density of 7.13 g/cm^3 is obtained at compaction pressure of 700 MPa. The green density of the compacts from EL powder mixtures is 7.11 g/cm^3 at the same pressure. When tungsten is introduced in the forms of elemental powders, the powder mixtures have low flowability and are easy to aggregate, resulting in the green density of powder compacts reducing. The prediffused Fe-W powders keeps the compressibility of reduced iron powder and the fine W powder sticks to the surface of iron powder, so the PD powder mixtures have better flowability and higher compressibility.

Density and Microstructure of the Sintered Fe-2Cu-0.8C-0.6Mo-2W Samples

Figure 3 shows density of the sintered Fe-2Cu-0.8C-0.6Mo-2W samples. With the increase of sintering temperature, density of sintered samples first increases, and then changes less. From **Figure 3**, it can be seen that when the sintering temperature is 1,150°C and sintering time is 90 min, the sintered samples
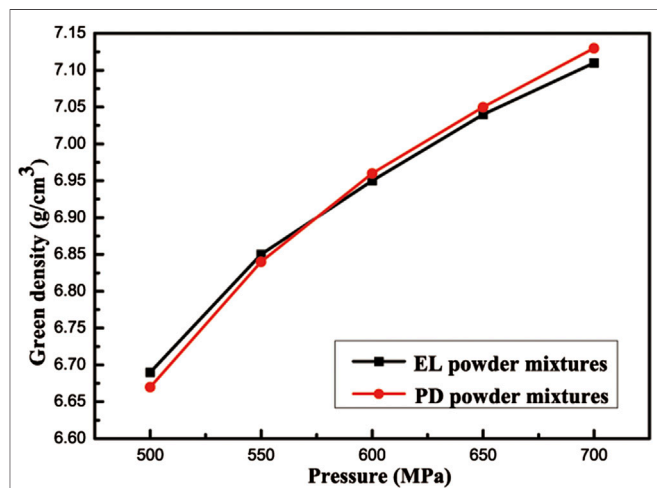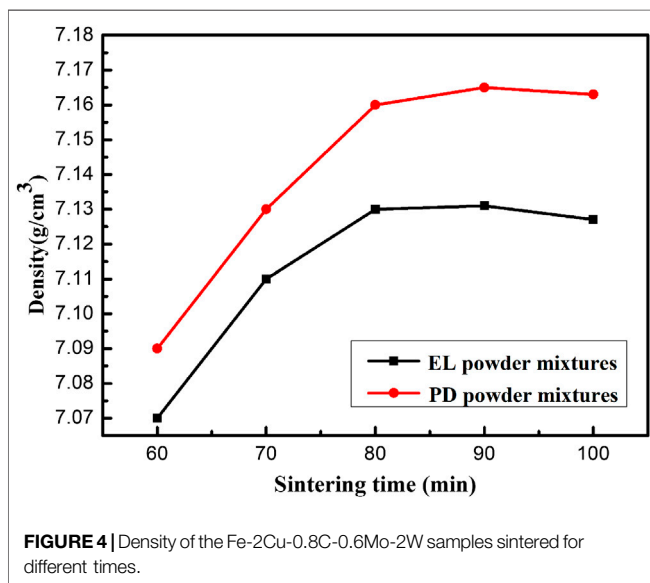

FIGURE 2 | Green density of the Fe-2Cu-0.8C-0.6Mo-2W compacts as a function of compaction pressure of 500–700 MPa.

FIGURE 3 | Density of the Fe-2Cu-0.8C-0.6Mo-2W samples sintered at different temperatures.
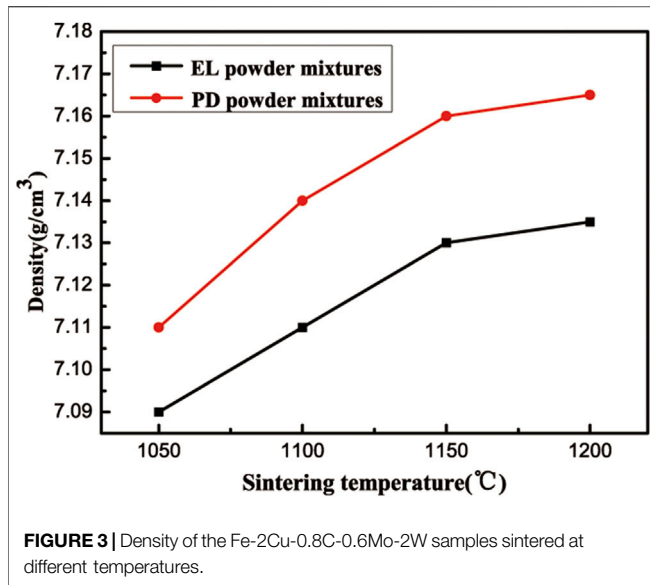
prepared from PD powder mixtures have a maximum density of 7.16 g/cm^3, while this value of EL powder mixtures is 7.13 g/cm^3. The advantage on density improvement of introducing W element in the form of prediffused Fe-W powder is proved again.

Figure 4 shows density of the samples sintering at 1,150°C for 60–100 min. It can be seen that with the increase of sintering time, density of sintered samples first increases and then remains unchanged, while the density of sintered samples from EL powder mixtures shows a slight decline. When the sintering time exceeds, not only the grain will grow abnormally, but also a small amount of copper would be lost, so the optimal of sintering time is also important. From **Figures 3**, **4**, it can be seen that the optimal sintering condition of Fe-2Cu-0.8C-0.6Mo-2W samples is 1,150°C for 90 min in H$_2$ atmosphere, and under this sintering

FIGURE 4 | Density of the Fe-2Cu-0.8C-0.6Mo-2W samples sintered for different times.

condition, samples prepared from PD powder mixtures have a higher density.

Figure 5 shows the morphology of the Fe-2Cu-0.8C-0.6Mo-2W samples with different addition forms of W sintered at 1,150°C for 90 min. **Figures 5A,B** present the morphology of sample prepared from EL powder mixtures, and **Figures 5C,**D correspond to the microstructure of that prepared from PD powder mixtures. The microstructure of the sintered sample from PD powder mixtures is more uniform with smaller grain size of ferrite (F) and pearlite (P), and the carbide is more evenly ferrite dispersed on the grain boundary. This microstructure effectively restricted the growth of pearlite, which is also critical for the performance of sintered iron-based materials.

Figure 6 shows the surface SEM image and EDS results of the samples sintering at 1,150°C for 90 min in H$_2$ atmosphere. Compared with samples prepared from EL powder mixtures (**Figures 6A,B**), the microstructure of sintered samples prepared from PD powder mixtures (**Figures 6C,**D) is more uniform, and the W element is better-distributed. Due to the adhesion of element W to iron particles before sintering, the diffusion of W element during the sintering densification process was improved. As the EDS results showing, W-rich region (WR) appeared in the sintered samples prepared from EL powder mixtures. By using PD powder mixtures, a diffusion layer between tungsten and iron before sintering is formed, which promote the diffusion of tungsten element during the sintering process. Different from other alloying elements for ferrous alloys like Ni, Cr, and Mn (formation of Ni (Cr, Mn)-rich ferrite), the microstructure of tungsten segregation area (W-Rich region (WR)) is blocky or granular in **Figure 6**.

Mechanical and Tribological Properties of Fe-2Cu-0.8C-0.6Mo-2W Samples

Figure 7 shows the effect of sintering temperature and time on tensile strength of sintered samples. With the increase of sintering temperature and time, tensile strength of sintered samples first increases, and then changes less. A maximum tensile strength of 547 MPa is obtained for the specimens from PD powder mixtures, sintered at 1,150°C and 90 min. When W element added in the form of prediffused Fe-W powder, the solid-state diffusion of W and Fe during sintering is promoted, thus the mechanical properties of sintered samples are improved. The diffusion and uniform distribution of the tungsten element improve the strength of matrix, so the sintered samples prepared from PD powder mixtures have a higher tensile strength.

The diffusion of alloying elements in the powder mixtures directly affects the tensile strength properties of the sintered material, and the improvement of properties is related to diffusion degree and densification during the sintering process. In this experiment, the tensile strength of the sintered materials can be considered as a function of the sintering temperature and time. A predictor is based on the following equation (Ddeoix et al., 2000):

$$f(t, T) = texp\left(-Q/RT\right) \qquad (1)$$
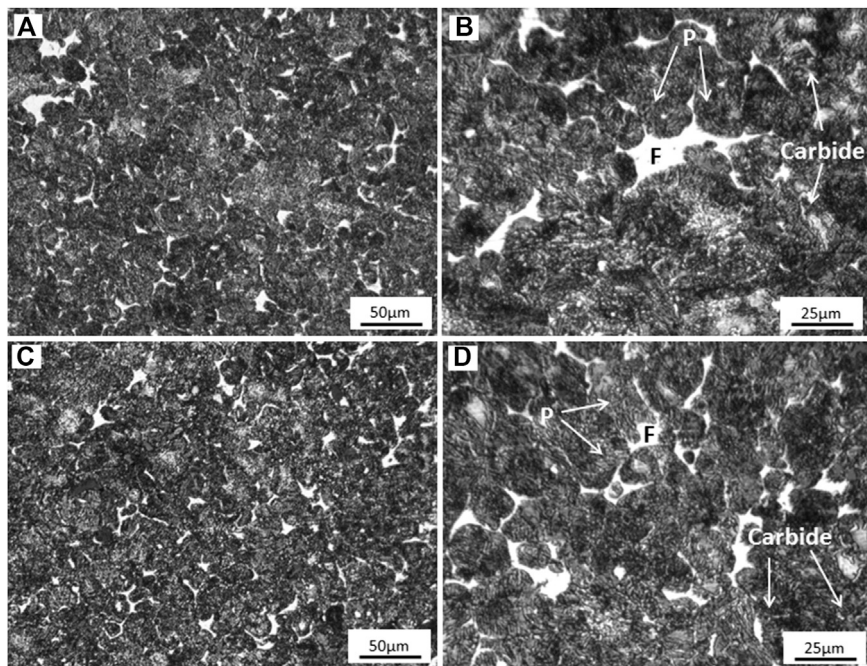
FIGURE 5 | Microstructure of sintered Fe-2Cu-0.8C-0.6Mo-2W materials from different powder mixtures. **(A**, **B)** EL powder mixtures; **(C**, **D)** PD powder mixtures
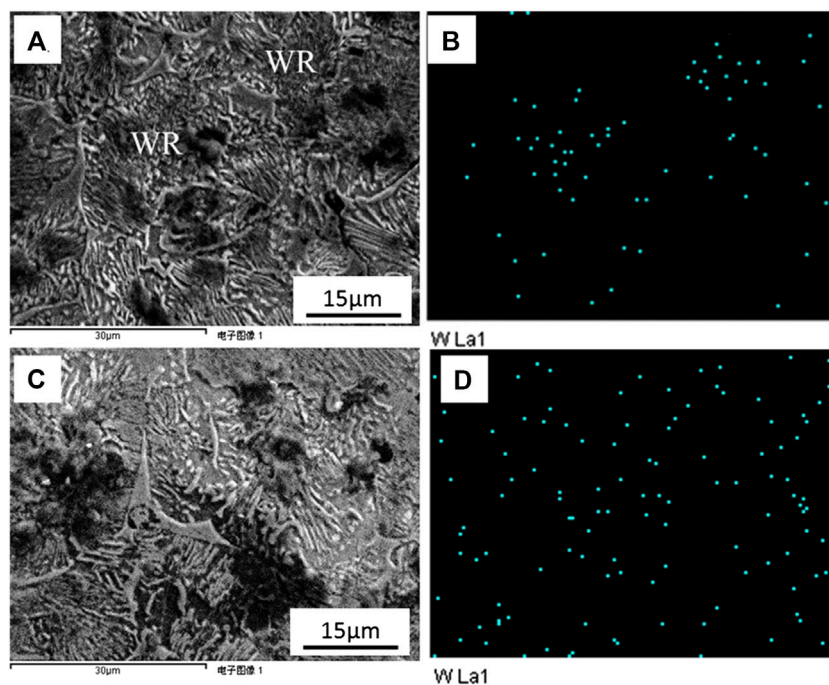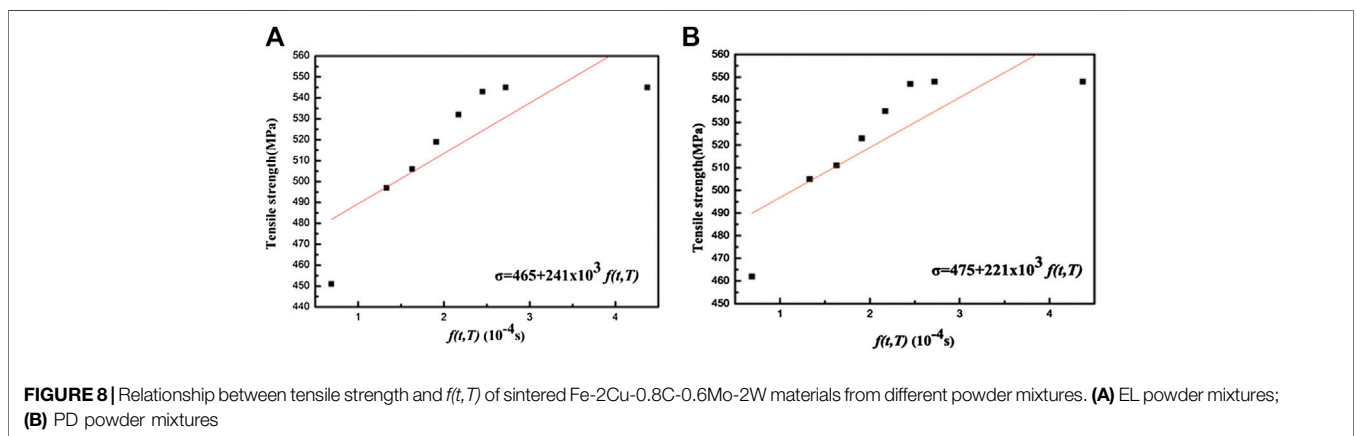

FIGURE 6 | SEM images and EDS results of sintered Fe-2Cu-0.8C-0.6Mo-2W materials from different powder mixtures. **(A**, **B)** EL powder mixtures; **(C**, **D)** PD powder mixtures

FIGURE 7 | Effect of sintering condition on tensile strength of sintered Fe-2Cu-0.8C-0.6Mo-2W samples. **(A)** sintering temperature; **(B)** sintering time.
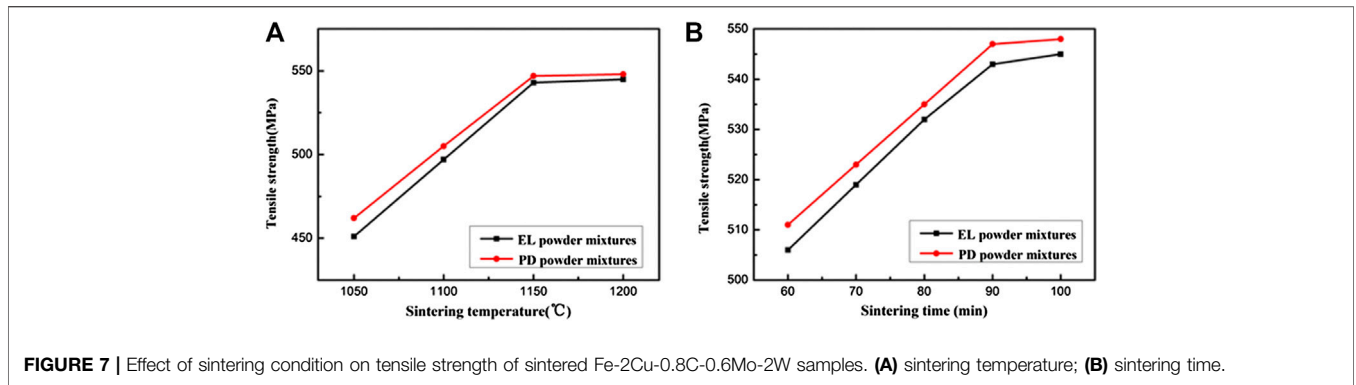
TABLE 1 | Value of $f(t, T)$.

Sintering condition	1,050°C 90 min	1,100°C 90 min	1,150°C 60 min	1,150°C 70 min	1,150°C 80 min	1,150°C 90 min	1,150°C 100 min	1,200°C 90 min
Value (s, 10^{-4})	0.69	1.33	1.63	1.91	2.17	2.45	2.72	4.37

FIGURE 8 | Relationship between tensile strength and $f(t,T)$ of sintered Fe-2Cu-0.8C-0.6Mo-2W materials from different powder mixtures. **(A)** EL powder mixtures; **(B)** PD powder mixtures

Where T is the sintering temperature (Kelvin), t is the sintering time, is the gas constant and the value is 8.314 J/(mol·K), and Q is the activation energy which was chosen to be 200 kJ/mol. **Table 1** shows the value of in this experiment.

Figure 8 shows the relationship between tensile strength and the function of sintered materials. The tensile strength (σ) of sintered samples sintered at 1,200°C for 90 min exists a big deviation mainly because of the abnormally grain growth with excessive sintering temperature. By analyzing the experimental data of the sintered samples prepared from EL powder mixtures and PD powder mixtures, **Eqs 2**, **3** are obtained respectively. These two equations allow the tensile strengths of different sintered samples to be estimated based on the sintering conditions. From the data, it can be found that within a reasonable sintering temperature range, with the increase of , the tensile strength of the sintered materials increases linearly.
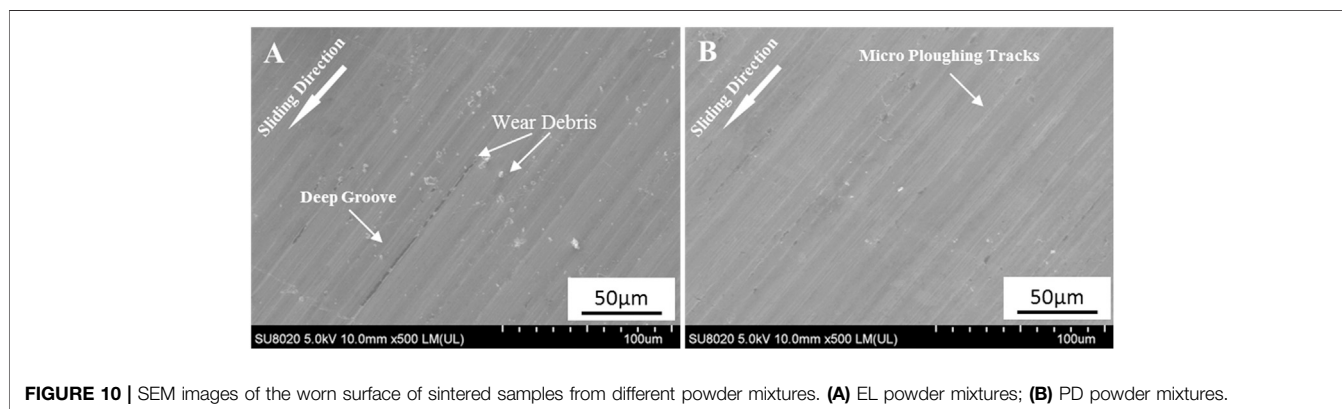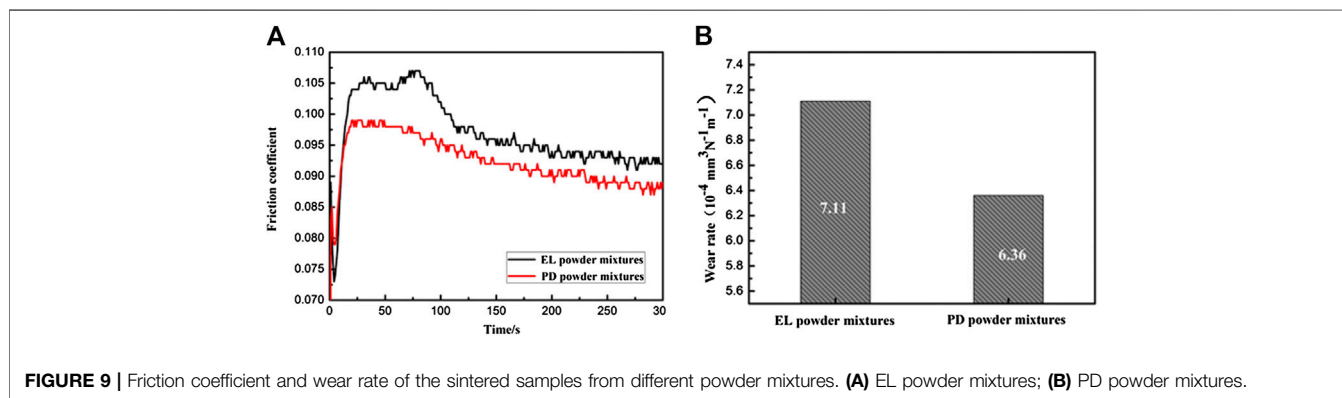
$$\sigma = 465 + 241 \times 10^3 f(t, T) \qquad (2)$$
$$\sigma = 475 + 221 \times 10^4 f(t, T) \qquad (3)$$

Table 2 lists the properties and comparison of Fe-2Cu-0.8C-0.6Mo-2W materials sintered at 1,150°C for 90 min. A maximum hardness of 95 HRB of the sintered samples were obtained from PD powder mixtures, higher than the value of MPIF standard and other Fe-Cu-C (W-containing) materials. A radial crushing strength of 791 MPa were obtained for the sintered samples from PD powder mixtures which the value of EL powder mixtures is 753 MPa. The diffusion of the tungsten can improve the hardness and strength of the matrix, and the tungsten carbide formed also can increase hardness, but for EL

TABLE 2 | Properties comparison of sintered Fe-2Cu-0.8C-0.6Mo-2W materials.

Composition	Density (g/cm³)	Tensile Strength (MPa)	Hardness (HRB)	Ref.
Fe-2Cu-0.8C-0.6Mo-2W (EL/PD powder mixtures)	7.13/7.16	543/547	93/95	This work
Fe-2Cu-0.8C	7.1	520	84	MPIF standard 35
Fe-2Cu-0.8C	7.14	410	59	3
Fe-1.5Cu-0.7C-1WC	6.63	317.3	72.6	8

FIGURE 9 | Friction coefficient and wear rate of the sintered samples from different powder mixtures. (A) EL powder mixtures; (B) PD powder mixtures.

FIGURE 10 | SEM images of the worn surface of sintered samples from different powder mixtures. (A) EL powder mixtures; (B) PD powder mixtures.

powder mixtures, the agglomerated carbides or W element will lead to stress concentration and elevate the brittleness.

The influence of W addition forms on coefficient of friction during the end-face wear test is shown in **Figure 9**. The coefficient of friction of the sample prepared from EL powder mixtures is 0.096, while the value of the sample prepared from PD powder mixtures is 0.092. Different microstructural features, hardness and strength values of the sintered samples lead to different friction behavior. The wear rate of the sample prepared from PD powder mixtures is 6.36×10^{-4} mm^3 $N^{-1}m^{-1}$ while the samples of the sample prepared from PD powder mixtures is 7.11×10^{-4} mm^3 $N^{-1}m^{-1}$. The sintered sample from PD powder mixtures shows uniform microstructure, higher hardness and lower value of coefficient of friction.

Figure 10 shows the worn surfaces of the sintered samples prepared from different powder mixtures. **Figures 10A** shows the worn surface of the sintered samples prepared by EL powder

mixtures, with some pores and deep grooves parallel to the sliding direction. The SEM image of the sintered samples from PD powder mixtures only shows some micro ploughing tracks on the worn surface (**Figures 10B**). The above features demonstrate that the tribological behavior improves by higher hardness and uniform microstructure.

The test results of tribological behavior show the samples prepared by adding PD powder mixtures own better properties. The reasons for forming abrasion scratch contain lubrication conditions, high contact stress and relative slip on the contact surface. The formula as following can be used to analyze the relationship between the hardness and wear property (Chen et al., 2003).

$$H = \frac{KWL}{CAP} \qquad (4)$$

Where H is the wear depth, is the friction coefficient relating to the wear condition of surface, W is the load on the sliding surface,

is the sliding distance, C is a constant, A is the contact area, and is the hardness of the contact surface. From the **Eq. 4**, it can be seen that the wear depth is directly proportional to the coefficient of friction, the size of load at each point on the contact surface and the sliding distance, but inversely proportional to the area of contact surface and hardness. With the increase of area and the hardness of the matrix, the adhesive wear reduced. With more diffusion during sintering after prediffused treatment for PD powder mixtures, the value of P is also improved.

CONCLUSION

Prediffused Fe-W powders were prepared using prediffused bonding treatments. The firmly metallurgical bonding between tungsten and iron particles could avoid the segregation of the W element. the optimal sintering condition was beneficial to sintering densification and the improvement of properties. When the sintering condition was 1,150°C for 90 min, a maximum tensile strength of 547 MPa, a hardness of 95 HRB and a radial crushing strength of 791 MPa were obtained for the specimens from PD powder mixtures, and the tribological behavior was also improved. The present results provided a potential way to improve the density and mechanical properties of ferrous powder metallurgy structure materials.

DATA AVAILABILITY STATEMENT

The original contributions presented in the study are included in the article/supplementary material, further inquiries can be directed to the corresponding author.

AUTHOR CONTRIBUTIONS

WC: designed and performed the experiments, manuscript draft and revising. JW: properties test. PC: experimental work, data analysis. JC: revised the manuscript, and final approval. All authors agree to be accountable for all aspects of the work.

ACKNOWLEDGMENTS

REFERENCES

Aditya, K., Peter, L., Magdalena, B., Dino, C., and Gaurav, S. (2015). On the application of inertial microfluidics for the size-based separation of polydisperse cementitious particulates. *Front. Mater.* 2, 48. doi:10.3389/fmats.2015.00048

Annamalai, R., Upadhyaya, A., and Agrawal, D. (2013). An investigation on microwave sintering of Fe, Fe–Cu and Fe–Cu–C alloys. *Bull. Mater. Sci.* 36 (3), 447–456. doi:10.1007/s12034-013-0477-9

Azevedo, J. M. C., Serrenho, A. C., and Allwood, J. M. (2018). Energy and material efficiency of steel powder metallurgy. *Powder Technol.* 328, 329–336. doi:10.1016/j.powtec.2018.01.009

Chawla, N., Murphy, T. F., Narasimhan, K. S., Koopman, M., and Chawla, K. K. (2001). Axial fatigue behavior of binder-treated versus diffusion alloyed powder metallurgy steels. *Mat. Sci. Eng. A* 308, 180–188. doi:10.1016/S0921-5093(00)01990-0

Chen, W. X., Tu, J. P., Wang, L. Y., Gan, H. Y., Xu, Z. D., and Zhang, X. B. (2003). Tribological application of carbon nanotubes in a metal-based composite coating and composites. *Carbon* 41, 215–222. doi:10.1016/S0008-6223(02)00265-8

Cristofolini, I., Molinari, A., Pederzini, G., and Rambelli, A. (2018). From experimental data, the mechanics relationships describing the behaviour of four different low alloyed steel powders during uniaxial cold compaction. *Powder Metall.* 61, 1–11. doi:10.1080/00325899.2017.1361507

Daumann, B., Weber, J. A., Anlauf, H., and Nirschl, H. (2011). Discontinuous powder mixing of nanoscale particles. *Chem. Eng. J.* 167, 377–387. doi:10.1016/j.cej.2010.12.033

Ddeoix, C. N., Griffo, A., and German, R. M. (2000). Effects of sintering parameters on the mechanical properties of a Fe-2Cu-2Ni-0.9M-0.8C steel. *Int. J. Mater. Prod. Technol.* 15, 409–426. doi:10.1504/ijmpt.2000.001248

Deng, X. T., Wang, Z. D., Han, Y., Zhao, H., and Wang, G. D. (2014). Microstructure and abrasive wear behavior of medium carbon low alloy martensitic abrasion resistant steel. *J. Iron Steel Res. Int.* 21, 98–103. doi:10.1016/S1006-706X(14)60015-7

Lee, J. G., Lim, C. H., Kim, H. S., Hong, S. J., Kim, M. T., Kang, B. C., et al. (2012). Highly dense steel components prepared by magnetic pulsed compaction of iron-based powders. *Powder Technol.* 228, 254–257. doi:10.1016/j.powtec.2012.05.027

Meng, H. J., Wang, J., Wang, L., Fang, X., Donga, N., Zhanga, C., et al. (2020). The precipitation control in aged alumina-forming austenitic stainless steels Fe-15Cr-25Ni-3Al-NbWCu by W addition and its effect on the mechanical properties. *Mater. Char.* 163, 110–233. doi:10.1016/j.matchar.2020.110233

Narasimhan, K. S. (2001). Sintering of powder mixtures and the growth of ferrous powder metallurgy. *Mater Chem Phys* 67, 56–65. doi:10.1016/S0254-0584(00)00420-X

Oka, S., Sahay, A., Wei, M., and Muzzio, F. (2017). Diminished segregation in continuous powder mixing. *Powder Technol.* 309, 79–88. doi:10.1016/j.powtec.2016.11.038

Pope, J. J., Calvert, E. L., Weston, N. S., and Jackson, M. (2019). FAST-DB: a novel solid-state approach for diffusion bonding dissimilar titanium alloy powders for next generation critical components. *J. Mater. Process. Technol.* 269, 573–599. doi:10.1016/j.jmatprotec.2019.02.011

Semel, F. J. (1990). Properties of parts made from an Ancorbond processed Fe-Ni-C powder mix. *Met. Powder Rep.* 45, 193–197. doi:10.1016/S0026-0657(10)80088-8

Silva, P. A., Weber, S., Inden, G., and Pyzalla, A. R. (2009). Influence of hard particle addition and chemical interdiffusion on the properties of hot extruded tool steel compounds. *Mater. Sci. Eng.* 516, 193–200. doi:10.1016/j.msea.2009.03.048.

Wang, X. D., Chen, Y. B., Wei, S. Z., Zuo, L. L., and Mao, F. (2019). Effect of carbon content on abrasive impact wear behavior of Cr-Si-Mn low alloy wear resistant cast steels. *Front. Mater.* 6, 153. doi:10.3389/fmats.2019.00153

Wu, M. W., Tsao, L. C., and Chang, S. Y. (2013). The influences of chromium addition and quenching treatment on the mechanical properties and fracture behaviors of diffusion-alloyed powder metal steels. *Mater. Sci. Eng.* 565, 196–202. doi:10.1016/j.msea.2012.12.032

Wu, Y. F., Hui, W. J., Chen, S. L., Xu, L., Yong, Q. L., and Zhou, S. T. (2016). Influence of vanadium on microstructure and mechanical properties of

medium carbon forging steel. *J. Iron Steel Res.* 28, 56–62. doi:10.13228/j.boyuan. issn1001-0963.20160073

Xiao, Z. Y., Ke, M. Y., Fang, L., Shao, M., and Li, Y. Y. (2009). Die wall lubricated warm compacting and sintering behaviors of pre-mixed Fe-Ni-Cu-Mo-C powders. *J. Mater. Process. Technol.* 209, 4527–4530. doi:10.1016/j.jmatprotec.2008.10.018

Xuan, Y., Hua, T., Ling, Q., and Yuxiang, L. (2019). Properties of Fe-Cu-C composite reinforced by different WC content[J]. *IOP MSE* 688, 033025. doi:10.1088/1757-899X/688/3/033025

Zhang, C., Li, P., Wei, S. Z., You, L., Wang, X., and Mao, F. (2019). Effect of tempering temperature on impact wear behavior of 30Cr3Mo2WNi hot-working die steel. *Front. Mater.* 6, 149. doi:10.3389/fmats.2019.0014